Food Research International 196 (2024) 115031

Contents lists available at ScienceDirect

Food Research International

journal homepage: www.elsevier.com/locate/foodres

Fabrication and characterization of whey protein isolate-tryptophan nanoparticles by pH-shifting combined with heat treatment

Lixin Yang [a,1], Hongmin Dong [a,1], Junyi Wang [a], Younas Dadmohammadi [a], Yufeng Zhou [a], Tiantian Lin [a], Waritsara Khongkomolsakul [a], Gopinathan Meletharayil [b], Rohit Kapoor [b], Alireza Abbaspourrad [a,*]

[a] Department of Food Science, College of Agricultural and Life Sciences, Cornell University, Ithaca, NY, 14853, USA
[b] Dairy Management Inc., Rosemont, IL, USA

ARTICLE INFO

Keywords:
Whey protein isolate
Tryptophan
Nanoparticles
pH-shifting
Thermal treatment

ABSTRACT

L-Tryptophan (Trp) is an essential amino acid with numerous health benefits. However, incorporating Trp into food products is limited due to its pronounced bitter taste. Encapsulating Trp in nanoparticles by using other natural biopolymers is a potential strategy to mask the bitter taste of Trp in the final products. Whey protein isolate (WPI), composed of alpha-lactalbumin (α-LA), bovine serum albumin (BSA), and beta-lactoglobulin (β-LG), has played a crucial role in delivering bioactive compounds. In order to incorporate Trp within WPI, the present study used a combination of pH-shifting and thermal treatment to fabricate whey protein isolate-tryptophan nanoparticles (WPI-Trp-NPs). During the pH-shifting technique, WPI unfolds at high pH, such as pH 11, and the dissociated WPI molecules are refolded when pH is shifted back to neutral, creating particles with uniform dispersion and encapsulating smaller particles surrounding them in solution. Further, the well-distributed nanoparticles formed by pH-shifting might encourage the formation of more uniform nanoparticles during subsequent thermal treatment. The WPI-Trp particles have an average particle size of 110.1 nm and a low average PDI of 0.20. Fluorescence spectroscopy confirmed the encapsulation of Trp by WPI, which shows higher fluorescence when the Trp is encapsulated by the WPI. Surface hydrophobicity, circular dichroism, particle size, free sulfhydryl, and antioxidant activity were used to characterize the WPI-Trp-NPs. WPI-Trp-NPs formed by pH-shifting combined with heating showed a higher surface hydrophobicity and free sulfhydryl content than the untreated WPI-Trp mixture. The conversion of α-helix into random coil in the WPI secondary structure indicated a more disordered structure of the modified whey protein. Molecular docking results indicate the interactions between Trp and WPI, including alpha-lactalbumin (α-LA), bovine serum albumin, and beta-lactoglobulin (β-LG), were mainly driven by hydrophobic interactions and hydrogen bonding. The binding affinity between Trp and these proteins was ranked as α-LA>BSA>β-LG. The combination of pH-shifting and heating improved the functionality of WPI and was an effective way to fabricate WPI-Trp nanoparticles.

1. Introduction

L-Tryptophan (Trp) is an essential amino acid obtained from dietary protein (Nongonierma & FitzGerald, 2015). Trp is a precursor for bioactive compounds such as nicotinamide, serotonin, melatonin, tryptamine, quinolinic, and xanthurenic acids and plays an important role in regulating appetite, mood, sleep, blood pressure, and sense of pain (Friedman, 2018; Nayak & Buttar, 2016). Trp and its metabolites are also related to the treatment of nervous system diseases and digestive system diseases (Xue et al., 2023). Despite the numerous health benefits, Trp has a pronounced bitter taste, making it less desirable as a food additive or supplement (Di Pizio & Nicoli, 2020).

Encapsulation is a commonly used technology in which different food ingredients such as caffeine and propolis are “entrapped” into the encapsulants to overcome the off-taste and improve the ingredients’ use in the food industry (Fuciños et al., 2017; Shakoury et al., 2022; Z. Zhang et al., 2020). Encapsulation of Trp has been reported in previous studies (Julieta et al., 2013; Rudolph et al., 2018). For instance,

* Corresponding author.
E-mail address: alireza@cornell.edu (A. Abbaspourrad).
[1] These two authors contributed equally to this manuscript.

https://doi.org/10.1016/j.foodres.2024.115031
Received 13 June 2024; Received in revised form 9 August 2024; Accepted 1 September 2024
Available online 3 September 2024

polymerization of liposomes was induced to encapsulate Trp through the UV irradiation of 1,2-bis(10,12-tricosadiynoyl)-*sn*-glyc-ero-3-phosphocholine (DC8,9PC) and 1,2-dimyristoyl-*sn*-glycero-3-phosphocholine (DMPC) (Julieta et al., 2013). However, this method involved the use of synthetic phospholipids, which limited the usage in food products with natural food ingredient labels. In another study, β-cyclodextrin was used to mask the bitterness of the Trp (Rudolph et al., 2018). However, the low solubility of β-cyclodextrin in the aqueous solution (Saokham et al., 2018) and the restricted intake amount (5 mg/kg body weight per day) could be a limitation for food product applications (Dong et al., 2024). To encapsulate Trp through natural food ingredients, we developed α-La-Trp nanoparticles by high-pressure homogenization combined with pH-shifting (Dong et al., 2024). Though the α-LA-Trp nanoparticles were successfully formed, scaling up this method proved challenging and costly considering the low amount of α-LA produced in the food industry. Therefore, a feasible method for the complexation of Trp with natural ingredients is still needed.

Whey protein isolate (WPI), a by-product of the dairy industry, is the main source of α-LA and could be an inexpensive and promising candidate for encapsulation of Trp. WPI, composed of β-lactoglobulin (β-LG), α-lactalbumin (α-LA), bovine serum albumin (BSA), immunoglobulins (IGs), and lactoferrin (LF), is known for its high nutritional value as well as its high binding properties to various biomolecules as an encapsulant (Li et al., 2015; Saberi Riseh et al., 2023; Salleh et al., 2022; Yi et al., 2016; Zhan et al., 2020; Zhao et al., 2022; Zhu et al., 2017). For example, whey protein has been used to encapsulate plant biocontrol bacteria, such as *Azospirillum lipoferum, Bacillus velezensis, and Pseudomonas putida.* These bacteria enhance the protection of plant products from pests and diseases (Li et al., 2015; Saberi Riseh et al., 2023; Salleh et al., 2022; Yi et al., 2016; Zhan et al., 2020; Zhao et al., 2022; Zhu et al., 2017). Whey protein nanoparticles were reported to encapsulate propolis extract with enhanced controlled release in gastrointestinal digestion (Shakoury et al., 2022). The interactions between whey protein nanoparticles and propolis extract include hydrophobic interaction and hydrogen bonding.

Various approaches have been investigated to use WPI for delivering bioactive compounds, including thermal treatments, pH modification, enzymatic treatments, etc. (W. Chen et al., 2019, p.; Ji et al., 2022; Salleh et al., 2022). Among these treatments, thermal treatment is frequently used as a straightforward processing treatment in the food industry. Whey protein aggregates with different structural types, such as microgels, fibrils, microparticles, and nanoparticles, can be made under specific pH, temperature, and ionic strength (Gołębiowski et al., 2020; Nicolai et al. 2011a; Ryan & Foegeding, 2015). It has been reported that WPI solution, upon thermal treatment, can unfold and expose interior hydrophobic groups and reactive sulfhydryl groups to the exterior of proteins. The exchange of free-SH groups and the formation of disulfide (S-S) bridges are thought to be responsible for the covalent bonding and cross-linking of nanoparticles (Jain et al., 2018; Ryan & Foegeding, 2015). Heat-induced nanoparticles containing more exposed hydrophobic groups are efficiently complex bioactive compounds such as soy isoflavones and curcumin and improve the bioaccessibility of biomolecules (Q. Liu et al., 2022; Mohammadian et al., 2020; C. Tang, 2021). Although heat-induced WPI nanoparticles proved promising in delivering bioactive compounds, limited information exists regarding the incorporation of Trp by heat-induced WPI nanoparticles.

Additionally, the functional and physicochemical properties of whey proteins can be altered using pH-shifting treatment. The pH-shifting treatment modifies the protein structure, and the resulting conformational changes improve protein dispersity, thermal stability, surface hydrophobicity, and emulsifying activity (W. Chen et al., 2019; J. Jiang et al., 2018; Z. Tang et al., 2021; Y. Wang et al. (2020), Zhang, et al., 2020). Previous studies have shown that pH-shifting treatment on whey proteins can encapsulate and deliver bioactive molecules with high binding activity, such as quercetin, carboxymethylcellulose, and (−)-epigallocatechin-3-gallate (EGCG) (C. Chen et al., 2022; W. Chen et al., 2019; Ding et al., 2023). Proteins can be unfolded at extremely high or low pH and refolded at neutral pH. Proteins, after pH-shifting, were found to be more unfolded with their hydrophobic residues exposed, and this led to a higher surface hydrophobicity (R. Wang et al., 2023). Natural WPI dispersed in solution remained a compact spherical structure with limited binding sites for Trp molecules. When the solution of the WPI-Trp mixture is adjusted to pH 11, the proteins in WPI unfold, exposing previously buried hydrophobic residues with which Trp can interact. When the pH of the solution is shifted back to neutral, the dissociated proteins refold, producing nanoparticles with a uniform size distribution. Despite several examples where pH shifting has been used effectively to change the functional properties of proteins, very few studies have used a combination of pH-shifting and heating on the formation of WPI nanoparticles for the incorporation of Trp.

Here, we aim to encapsulate Trp in WPI nanoparticles using a combination of pH-shifting and thermal treatment. We hypothesize that the unfolding and refolding process during pH shifting promotes the complexation of WPI with Trp and facilitates the homogeneous dispersion of the WPI-Trp mixture. This process may aid in forming more uniform nanoparticles during subsequent thermal treatment. Experimental conditions, such as pH, heating temperature, and heating time, were optimized to find the best conditions to encapsulate Trp in WPI nanoparticles. These nanoparticles were then characterized, and the interaction mechanism between WPI and Trp was investigated using intrinsic fluorescence, surface hydrophobicity, free sulfhydryl group, circular dichroism, radical scavenging capacity, and FTIR. The fabricated WPI-Trp nanoparticles could be used as a functional ingredient in the food industry that may mask the bitter taste of Trp.

2. Materials and methods

2.1. Materials

Whey protein isolate powder (Provon 190) was provided by Glanbia Nationals, Inc (Fitchburg, WI, USA). Tryptophan (Trp, reagent grade > 98 %), 2,2-diphenyl-1-picrylhydrazyl (DPPH, reagent grade > 97 %), 2,2-azinobis (3-ethylbenzothiazoline-6-sulfonic acid (ABTS, reagent grade > 98 %), 8-anilino-1-naphthalenesulfonic acid (ANS, reagent grade > 98 %), were purchased from Sigma-Aldrich (10417, St Louis, MO, USA). 5,5′-Dithiobis-(2-nitrobenzoic acid) (DTNB) was purchased from ThermoFisher (02451, Waltham, MA, USA) Hydrochloric acid (reagent grade > 37 %), and sodium hydroxide (reagent grade > 97 %) were purchased from Fisher Scientific (Hampton, NH, USA). Milli-Q water was prepared from a Millipore water purification system (Millipore Sigma, Burlington, MA, USA). All the other chemicals used in this study were analytical grade.

2.2. Preparation of whey protein-Tryptophan nanoparticles (WPI-Trp NPs)

2.2.1. pH-shifting treatment

The WPI-Trp solution was prepared by dissolving WPI and Trp powder samples in a 5:1 ratio (w/w) in Milli-Q water with magnetic stirring (800 rpm) for 2 h. The WPI-Trp solution was stored in a refrigerator (4 °C) for 12 h to ensure complete hydration. Next, the WPI-Trp solution was adjusted to pH 11 with 1 mol/L NaOH and was stirred at 800 rpm for 1 h. Then, the WPI-Trp solution at pH 11 was divided into three parts and the pH readjusted into pH 5, 6, and 7 with 1 mol/L HCl and stirred at 800 rpm for another hour. The resultant WPI-Trp solutions were adjusted to a final concentration of 2.5 w/v % with Milli-Q water to produce the pH-shifted WPI-Trp stock solution. The WPI-Trp solution without pH-shifting was divided into three parts and adjusted to pH 5, 6, and 7 with 1 mol/L HCl, respectively, with a final concentration of 2.5 w/v %.

Control solutions of WPI and Trp with and without pH-shifting were produced using the same protocol.

2.2.2. Heat treatment on pH-shifting samples

For the pH-shifting combined with heating samples, aliquots of 2 mL pH-shifted WPI-Trp, WPI, and Trp sample solutions (2.5 w/v %) were filled into glass tubes separately and placed in a constant-temperature (50, 60, 70, 80 °C) water bath (Model WB20, VWR International) and heated for 10, 20, 30, 40, 50, and 60 min, respectively to induce heat-induced nanoparticles. The heat treatment was terminated by putting these glass tubes in an ice bath for 4 min to room temperature.

2.3. Characterization of WPI-Trp NPs

2.3.1. Particle size analysis

Particle size measurements were conducted to investigate the effect of pH-shifting and heat treatment on protein aggregation. The WPI-Trp, WPI, and Trp nanoparticles were analyzed for their average diameter, particle size distribution, and polydispersity index (PDI) using dynamic light scattering instruments (Zetasizer Nano-ZS, Malvern, UK). The analyses were performed at 25 °C in a cuvette with a 1 cm path. The measurements were repeated at least six times and in triplicate for each analysis.

2.3.2. Circular dichroism (CD) spectroscopy analysis

CD spectroscopy was conducted using an AVIV-202–01 spectropolarimeter (Lakewood, NJ, USA) to investigate the secondary structure changes of WPI, and WPI-Trp samples after thermal treatment and pH-shifting. CD spectra were measured with a wavelength of 190–260 nm at 25 °C. Samples with a concentration of 2 mg/mL were measured in a 1-mm-path quartz cell. Web-based DichroWeb was used to calculate the secondary structures of samples (https://dichroweb.cryst.bbk.ac.uk/html/home.shtml).

2.3.3. Intrinsic fluorescence

Intrinsic fluorescence spectra were carried out to study the aggregation-induced effect between WPI and Trp and the dynamic structure change of WPI. The intrinsic fluorescence of all the fabricated WPI-Trp, WPI, and Trp samples was recorded at room temperature using a fluorescence spectrophotometer (Hitachi, F-7000, Japan). The fluorescence emission spectra of the samples were excited at 295 nm and recorded from 310 to 500 nm (Zhan et al., 2020).

2.3.4. Surface hydrophobicity

Surface hydrophobicity measurements were conducted to investigate the protein conformational change during pH-shifting and heating. Surface hydrophobicity was detected using ANS as a fluorescence probe (H. Jiang et al., 2022). The ANS stock solution (8.0 mM) was prepared in a phosphate buffer (10 mM, pH 7.4). Six sample concentrations were prepared with the above buffer from 0.01 mg/mL to 0.25 mg/mL. Next, 2 μL of ANS was added to 200 μL of WPI alone and the WPI-Trp mixture, with and without treatments (5:1, w/w) in a 96-well plate separately. Then, the plate was kept in the dark for 20 min before reading on a microplate reader (SpectraMax iD3, Molecular Devices, San Jose, CA, USA) with an excitation wavelength and an emission wavelength of 390 nm and 470 nm, respectively. The sample's surface hydrophobicity (H_0) was calculated as the slope of the curve of fluorescence intensity against sample concentration.

2.3.5. Turbidity

Turbidity was measured to analyze the development of protein aggregation during pH-shifting and heating. The turbidity of WPI, Trp, and WPI-Trp was measured according to the previous method (Lin et al., 2022).

2.3.6. Fourier transform infrared spectroscopy (FTIR)

FTIR spectra were conducted to analyze the driving force for the formation of the WPI-Trp nanoparticles. The FTIR spectra of freeze-dried WPI, WPI-Trp, and Trp powder samples were recorded using the FTIR spectrometer (Shimadzu Instrument, Kyoto, Japan) in the range of 4000 cm^{-1} to 400 cm^{-1} wavenumbers. The measurement was taken in an average of 32 scans at a resolution of 4 cm^{-1}.

2.3.7. Scanning electron microscopy (SEM)

The microstructure of the freeze-dried samples (WPI-Trp mixture at pH 6, WPI-Trp mixture after heating, WPI-Trp mixture with pH-shifting and WPI-Trp mixture with pH-shifting and heating)and solution samples before freeze-drying (WPI-Trp mixture before freeze-drying and WPI-Trp-NPs) was imaged using the SEM (Zeiss Gemini 500, Jena, Germany). Samples were vacuum-dried before scanning and imaging in the SEM. SEM analysis was done according to the previous method (Lin et al., 2022).

2.4. Antioxidant activity

2.4.1. DPPH radical scavenging capacity

The DPPH radical scavenging activity of the fabricated WPI, Trp, and WPI-Trp samples was measured according to a previously published method (Dong et al., 2016) with a slight modification. The DPPH solution was dissolved in pure ethanol with a concentration of 0.2 mmol/L. The modifications are as follows: samples were diluted with Milli-Q water to various concentrations: 0.5 mg/mL, 1 mg/mL, 2 mg/mL, and 5 mg/mL. Next, 200 μl of sample was mixed with 100 μL of DPPH solution (0.2 mmol/L), and the mixture was stored in darkness for 30 min at room temperature before the absorbance was recorded at 517 nm (~25 °°C). The DPPH radical scavenging capacity was calculated using the following equation:

$$Radicalscavengingcapacity(\%) = \frac{A0 - (A1 - A2)}{A0} \times 100\% \quad (1)$$

Where A_0 is the absorbance of the control group (DPPH solution with Milli-Q water), A_1 is the absorbance of the sample group (DPPH solution with sample solution), A_2 is the absorbance of the sample blank group (sample solution with ethanol).

2.4.2. ABTS radical scavenging capacity

ABTS radical scavenging capacity was measured according to the previously published protocol with some modifications (Dong et al., 2016). The modifications are as follows: samples were dissolved in phosphate buffer (pH 7.4) to a concentration of 0.05 mg/mL. Next, a 20 μL aliquot of the sample was mixed with 200 μL of the ABTS working solution, and the mixture was stored in the dark for 20 min at room temperature before the absorbance was recorded at 734 nm (~25 °C). The ABTS radical scavenging capacity was calculated using Eq (1), where A_0 is the absorbance of the control group (ABTS solution phosphate buffer), A_1 is the absorbance of the sample group (ABTS solution with sample solution), A_2 is the absorbance of sample blank group (sample solution with water).

2.5. Sulfhydryl group content (SH)

The free sulfhydryl group content of WPI and WPI-Trp samples was measured according to a previously published method (Z. Jiang et al., 2022). The mixture of samples with DTNB was considered as the sample group, and samples without DTNB were considered as the sample blank. The mixture of Tris-Gly buffer with DTNB was considered as the reagent blank. The absorbance value of the mixture was recorded at 412 nm with a UV–Vis spectrophotometer (UV-2600, SHIMADZU Co., Japan). The content of free sulfhydryl groups was calculated according to the following equation:

$$SH(\mu M/L) = \frac{(A_{412} \times 73.53 \times D)}{C} \quad (2)$$

Where A_{412} is the absorbance at 412 nm, C is the sample concentration,

and D is the dilution factor.

2.6. Molecular docking

Molecular docking was conducted to further understand the interaction mechanism of whey protein and Trp. Auto Dock Vina 1.2.0 software (Trott & Olson, 2009) was performed to predict the interaction between whey protein and Trp. The 3D crystal structure of α-LA (PDB: 1F6R), β-LG (PDB: 3NPO), and BSA (PDB: 4F5S) were obtained from Protein Data Bank (https://www.rcsb.org/) acting as receptor molecules that merge nonpolar hydrogens and incorporate charges. Blind docking was conducted to predict the lowest energy binding sites for Trp on α-LA, β-LG, and BSA. PyMOL *ver.* 2.5.2 software was used to visualize the docking results and the interactions between the ligand and receptor were analyzed by Ligplot (Wallace et al., 1995).

2.7. Data and statistical analysis

All data were analyzed and plotted by two software, JMP (version Pro15, SAS, USA) and GraphPad Prism9 (GraphPad Software Inc., USA). All the experiments were conducted in triplicate, and the mean value with standard deviation was expressed in the graphs. ANOVA and Tukey HSD comparison test ($p < 0.05$) were used to analyze the sample differences.

3. Results and Discussion

WPI-Trp nanoparticles were fabricated using pH-shifting followed by thermal treatments. The WPI-Trp NPs were then fully characterized. Finally, a mechanism for the formation of the nanoparticles is proposed.

3.1. Effect of pH shifting on the formation of WPI-Trp nanoparticles (WPI-Trp NPs)

To determine the effect of pH-shifting on the formation of WPI-Trp NPs, 2.5 w/v % solutions of WPI and Trp were mixed at a ratio of 5:1 (w/w) were dissolved in an alkaline solution at pH 11 and then shifted back to pH 5, 6, and 7, respectively, followed by heating at 70 °C for 1 h. After pH-shifting and heating, the pH 11–5 WPI-Trp sample showed undesirable precipitation, which did not satisfy the nanoparticle design requirement (Fig. 1A). Aggregation can occur at pH 5 even at room temperature because pH 5 is close to the isoelectric point of WPI (pI ≈5.1) (Nicolai et al., 2011b), then heating enhances this aggregation. When the pH is shifted from 11 to 6 or 11 to 7, mixtures of WPI-Trp showed the formation of nanoparticles (Fig. 1B). The particle sizes of WPI-Trp NPs obtained under pH-shifting (from 11 to 7 and 11 to 6), and pH-shifting combined heat treatment (pH-shifting from 11 to 7 and 6 combined with heating under 70 °C for 1 h) ranged from less than 50.0 nm to the largest particles size of 156.0 ± 3.0 nm when the pH was shifted from 11 to 6 followed by heating (Fig. 1B). We attribute this to the pH being near the *iso*-electric point of WPI and the electrostatic repulsion was low (Y. Liu et al., 2018; Yu et al., 2020). Shifting the pH from 11 to 7 followed by heating did not significantly increase ($p > 0.05$) the size of WPI-Trp, and the particles were smaller than the samples shifting from pH 11 to 6 followed by heating. This difference in size may be due to the heat-induced aggregation influence was much weaker at a pH further away from the isoelectric point.

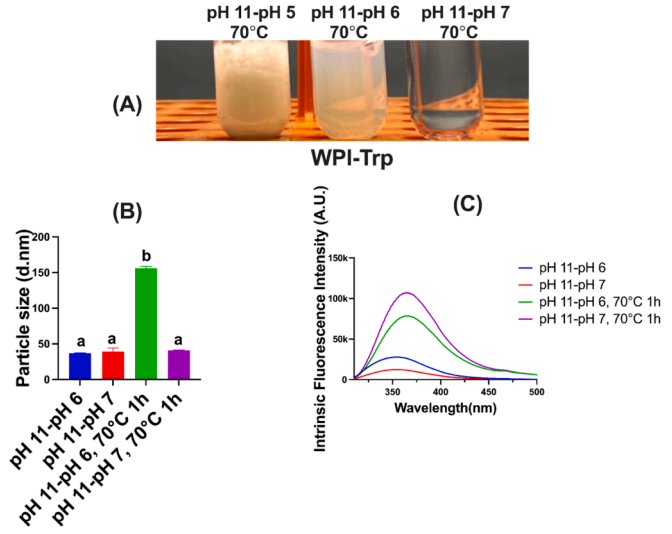

Fig. 1. Effect of pH-shifting on the formation of WPI-Trp (A) Image of WPI-Trp mixture, (B) Particle size of WPI-Trp mixture, and (C) Intrinsic fluorescence spectra of WPI-Trp mixture. Different letters indicate a significant difference ($p < 0.05$).

Intrinsic fluorescence has been considered an effective approach to studying the conformational changes of proteins (Samanta et al., 2000). Tryptophan is one of the main fluorophores of protein, and the binding characteristics of Trp are studied by recording the fluorescence spectra emission at specific excitation wavelengths (Bromley et al., 2006). The emission of Trp can be strongly quenched, or non-fluorescent, when they are free dispersed in a buffer due to the rapid nonradiative decay via twisted-intramolecular charge transfer (TIFT) (Scheme. 1). Aggregation-induced emission is observed when a fluorescent molecule is trapped in the protein aggregates, as the rotation of the fluorescencing molecule is restrained. The restricted intermolecular movement results in a reduction of TIFT (De et al., 2021; Y. Liu et al., 2018; Yu et al., 2020). Therefore, the intrinsic fluorescence intensity of Trp is positively related to the encapsulated Trp content in protein aggregates and can be used to characterize WPI-Trp nanoparticles.

The fluorescence spectra of the WPI-Trp sample that was pH shifted from 11 to 6 showed a higher intrinsic fluorescence intensity than the sample that was pH shifted from 11 to 7 (Fig. 1C). This suggested that a higher content of Trp was trapped in the samples obtained by shifting from pH 11 to pH 6, based on the aggregation-induced emission theory, which has shown that higher content of trapped fluorescent Trp is positively related to a higher intrinsic Trp fluorescence intensity (Y. Liu et al., 2018; Yu et al., 2020).

WPI-Trp of the sample shifted from pH 11 to pH 6 and then heated at 70 °C showed a higher intrinsic intensity compared to the heated or unheated pH 11 to pH 7 sample as well as the unheated pH 11 to pH 6 sample, which is related to the formation of WPI-Trp nanoparticles with higher amount of Trp loaded. The increase of maximum emission wavelength from ~350 nm of the unheated samples to ~360 nm of heated samples also indicated that a higher number of Trp molecules were entrapped within the protein aggregates after heating. This increase in the maximum emission wavelength phenomenon was also reported in a previous study when Trp molecules were incorporated

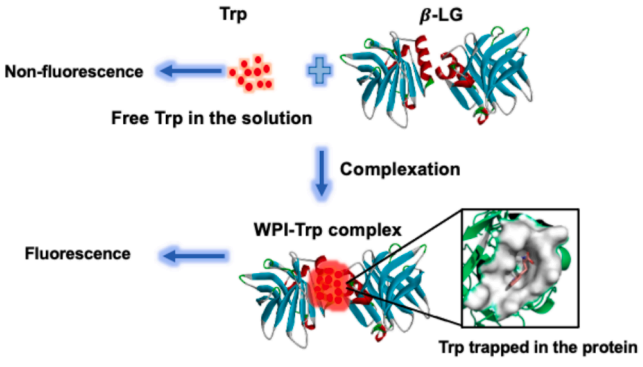

Scheme 1. Proposed mechanism of the aggregation-induced emission.

within the α-LA proteins (Dong et al., 2024).

3.2. Effect of heating temperature on the formation of WPI-Trp NPs

Heating temperature is one of the primary factors that can influence protein particle size (Raikos, 2010). Previous studies showed that the denaturation temperature of WPI is between 65 and 70 °C (L. Zhang et al., 2021). Specifically, β-LG has shown a denaturation temperature at 70 °C at neutral pH (De Wit, 2009), α-LA has an average denaturation temperature at 63.7 °C (McGuffey et al., 2005), and the BSA was reported to denature at 330 K (56.85 °C) (Matsarskaia et al., 2020). The heating temperature can affect the extent of protein denaturation (Wouters et al., 2022). Denatured proteins with exposed hydrophobic residues and reactive sulfhydryl groups are prone to result in hydrophobic interactions and form disulfide bonds between protein particles (Monahan et al., 1995; Wouters et al., 2022). In our samples, higher temperature caused larger particles to form between WPI and Trp in a range from 38.9 ± 0.6 nm at 50 °C to 341.1 ± 5.1 nm at 80 °C (Fig. 2A). When WPI-Trp was pH shifted from pH 11 to 6 followed by heating at 80 °C for 1 h produced the largest sized particles among the three temperature groups due to heat-induced aggregation. It has been reported that whey proteins unfold and expose additional hydrophobic groups when heated above 65 °C (Raikos, 2010), and the level of protein denaturation is positively related to the heating temperature, which is reflected in the fluorescence spectra. Increasing the temperature resulted in a red shift in the fluorescence spectra, indicating that the proteins unfolded further upon increasing the temperature, and more interior amino acid groups were exposed (Z. Jiang et al., 2022; Sun et al., 2022). Consequently, these exposed hydrophobic groups interacted with additional Trp molecules, which might contribute to particle aggregation (Nicolai et al. 2011a). The fluorescence intensity of WPI-Trp heated at 70 °C was the highest (Fig. 2C), and this increase suggests the greatest complexation of Trp with WPI. The fluorescence intensity decreased at 80 °C, which is most likely due to a higher content of proteins that were unfolded followed by a strong hydrophobic interaction between proteins that limited the Trp incorporation. In contrast, at 50 °C and 60 °C, there was less protein unfolding and aggregation, and therefore, a lack of exposed hydrophobic residues limited the encapsulation of Trp. This was observed by the lower intrinsic fluorescence intensity of WPI-Trp heated at 50 °C and 60 °C (Fig. 2C).

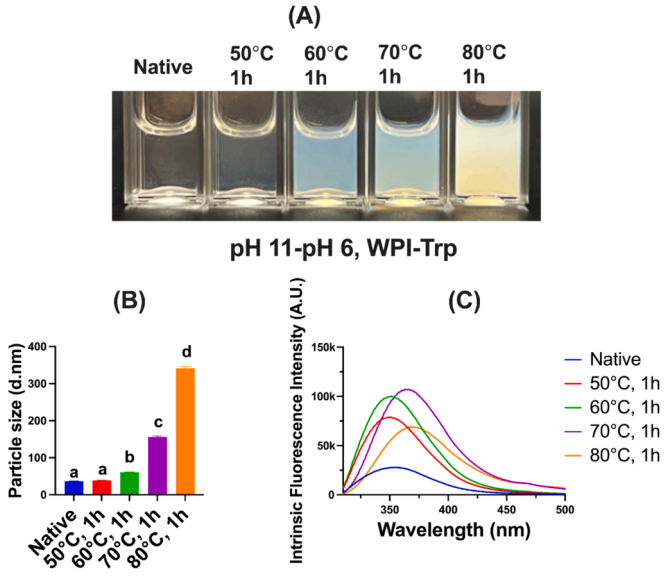

Fig. 2. Effect of temperature on the formation of pH 11-pH 6, WPI-Trp (A) Image of pH-shifting WPI-Trp mixture heated at 50/60/70/80 °C (B) Particle size of pH-shifting WPI-Trp mixture heated at 50/60/70/80 °C, and (C) Intrinsic fluorescence spectra of pH-shifting WPI-Trp mixture heated at 50/60/70/80 °C.

3.3. Effect of heating time on the formation of WPI-Trp NPs

In addition to the temperature of heat treatments, heating time also influences protein aggregation (Raikos, 2010). One of the primary indicators of the development of protein aggregation is turbidity. Both turbidity and particle size of the non-pH-shifted group and the pH-shifted group increased with longer heating times due to heat-induced aggregation. Extended heating time resulted in higher levels of aggregation of particles with increased size and turbidity (Fig. S1). WPI-Trp samples without pH-shifting demonstrated significantly higher turbidity and larger particle sizes than samples obtained after pH-shifting ($p < 0.05$), and precipitates were observed. Heat-induced aggregation was more significant in samples without pH-shifting, while WPI-Trp samples after pH-shifting had reduced sensitivity to thermal aggregation. The difference in turbidity and particle size upon heating between WPI-Trp with pH-shifting and WPI-Trp samples without pH-shifting can be explained by the modification of the WPI structure during pH-shifting. Recent studies have demonstrated that pH-shifting can induce protein unfolding and refolding, which modifies the natural protein structure causing a molten-globule state with a looser tertiary structure. WPI in the molten-globule state would have an enhanced interaction with water, which explains why it appears to be less turbid than WPI without pH-shifting (Z. Jiang et al., 2022). In the molten-globule state, the originally compact structure of WPI is disrupted, and the flexibility of the protein structure is enhanced (W. Chen et al., 2019; J. Jiang et al., 2010; Z. Jiang et al., 2022). The increased flexibility of the protein structure in the molten-globule state may be helpful in reducing the heat-induced aggregation effect. The disruption of disulfide bonding of pH-shifted WPI (Z. Jiang et al., 2022) and the strong electrostatic repulsion between protein molecules during pH-shifting might also contribute to the reduced heat-induced aggregation level compared with the WPI without pH-shifting (W. Chen et al., 2019; Ding et al., 2023; Igartúa et al., 2024). Upon heating, WPI-Trp demonstrated a greater particle size and turbidity than WPI alone, indicating that the WPI aggregation was enhanced in the presence of Trp. We attribute this to the increased interaction between the exposed hydrophobic residues on WPI with Trp. Previous studies also showed similar phenomena. The binding of α-LA with Vitamin D_3 contributed to larger particle size due to interactions between exposed hydrophobic patches of α-LA and Vitamin D_3 (Delavari et al., 2015).

The fluorescence intensity of the WPI-Trp mixture reached its highest after 20 min of heat treatment (Fig. 3A). Heating longer than 20 min caused the fluorescence intensity to decrease and was accompanied by a slight red shift. This was attributed to the limited access of Trp to the interior of the protein due to strong protein–protein interaction resulting from extended heating times. Upon heating, the intrinsic fluorescence intensity of WPI samples that were pH-shifted increased during 30 min heating with a fluorescence emission maximum (λ_{max}) over 350 nm. Tryptophan molecules on proteins are fully exposed to aqueous buffer when the λ_{max} is over 350 nm (Grossmann et al., 2019). Aggregation of protein molecules induced by heating led to reduced solvent quenching of the Trp fluorescence, resulting in an increase in the Trp fluorescence intensity. (Fig. 3B) (Bhattacharya et al., 2011; Geddes, 2016; C. Wang et al., 2022). After 30 min of heating, the fluorescence intensity began to decrease. The Trp fluorescence quenching could be due to the changes in the proximal amino acids and disulfides that occurred during aggregation (Bhattacharya et al., 2011; Geddes, 2016). The intrinsic fluorescence intensity of Trp remained much lower than WPI and WPI-Trp samples (Fig. 3C). Based on the aggregation-induced emission, a strong quenching effect would reduce the fluorescence emission when Trp molecules were freely dispersed in a hydrophilic environment (Royer, 2006).

Natural WPI-Trp at pH 6 had a particle size of 68.2 ± 2.1 nm, which decreased to 36.8 ± 0.6 nm after pH-shifting treatment and a slight

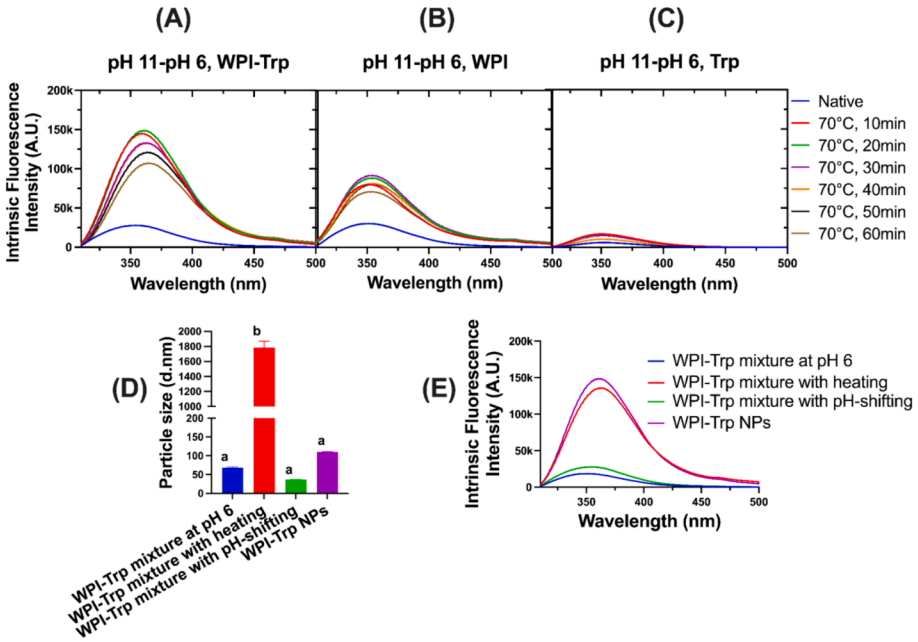

Fig. 3. Intrinsic fluorescence spectra of pH 11-pH 6, 70 °C, 0–60 min, (A) WPI-Trp/ (B) WPI/ (C) Trp; (D) Particle size of WPI-Trp mixture at pH 6, WPI-Trp mixture with heating at 70 °Cfor 20 min, WPI-Trp mixture with pH-shifting, and WPI-Trp NPs with pH-shifting combined with heating at 70 °C for 20 min, and (E) Intrinsic fluorescence spectra of WPI-Trp mixture at pH 6, WPI-Trp mixture with heating at 70 °C for 20 min, WPI-Trp mixture with pH-shifting, and WPI-Trp NPs with pH-shifting combined with heating at 70 °C for 20 min. Different letters indicate a significant difference ($p < 0.05$).

increase in the intrinsic intensity accompanied by a red shift (Fig. 3D and E). Similar findings were reported where WPI exhibited a smaller and more uniform size distribution after undergoing pH-shifting treatment (Ding et al., 2023). Additionally, whey protein after pH-shifting demonstrated a molten-globule state with a more flexible and unfolded structure. Hydrophobic residues and inner fluorophores, Tyrosine, Tryptophan, and Phenylalanine were exposed. The exposure of inner fluorophores as well as a higher amount of loaded Trp resulted in a higher fluorescence intensity.

WPI-Trp that was not pH-shifted but heated resulted in large particle sizes of 1784.0 ± 85.4 nm, where the heat-induced protein aggregation effect was substantial. While the pH-shifted and then heated WPI-Trp solutions showed a significantly smaller size at 110.1 ± 0.8 nm ($p < 0.05$), which indicated that pH-shifting caused the WPI-Trp particles to be less thermally sensitive. Further, pH-shifting combined with heating WPI-Trp had the highest fluorescence intensity, and the heating-only sample had a slightly lower peak (Fig. 3E). It was believed that both heat and pH-shifting treatment functionalized whey protein and contributed to Trp complexation.

3.4. Characterization of WPI-Trp NPs produced at optimized conditions

Based upon our data we chose pH shifting from pH 11 to pH 6 followed by heating at 70 °C for 20 min as the optimized conditions to fabricate WPI-Trp nanoparticles. Under these conditions, the fluorescence intensity reached a maximum and the size of the nanoparticles was 110.1 ± 0.8 nm with low PDI (0.20 ± 0.02), which satisfied the requirements to be considered nanoparticles.

3.4.1. SEM imaging

The microstructure of WPI-Trp with different processing treatments was analyzed using SEM (Fig. 4). The WPI-Trp sample at pH 6 after freeze-drying (FD) demonstrated large-scale flakes. It was suggested that freeze-drying the samples caused further aggregation on the sample (Roy & Gupta, 2004). Compared to the untreated sample, the WPI-Trp sample that was heated without pH-shifting showed a greater level of aggregation and conjugation (Fig. 4B). The freeze-dried WPI-Trp sample with pH-shifting (Fig. 4C) showed rod-like shape. For freeze-dried WPI-Trp NPs samples obtained by pH-shifting combined with heating (Fig. 4D), square-like aggregates were formed and evenly distributed with similar sizes, which suggested that the pH-shifting samples self-aggregated to a more compact whey protein structure after heating (Fig. 4D). However, the size of freeze-dried WPI-Trp NPs was larger than the WPI-Trp NPs without freeze-drying (Fig. 4F), suggesting that freeze-drying caused the further aggregation (Roy & Gupta, 2004). The solution WPI-Trp NPs samples (before freeze-drying) with pH-shifting combined with heating (Fig. 4F) showed evenly distributed nanoparticles with a spherical shape, while the solution samples prepared without pH-shifting treatment but were heat treated (Fig. 4E) showed dense and large aggregates, which was consistent with the particle size distribution, in which the heating alone WPI-Trp showed significantly larger particle sizes. Based on the difference in microstructure, we confirmed that the sample with pH-shifting showed less thermal sensitivity compared to samples without pH-shifting and confirmed the formation of WPI-Trp. NPs by combining pH-shifting (pH from 11 to 6) and heat treatment (70 °C, 20 min).

3.4.2. Surface hydrophobicity

The surface hydrophobicity (H_0) of the protein indicates how many hydrophobic groups are exposed to the protein surface (Y. Wang et al. (2020), Yang, et al., 2020). The pH-shifting treatment significantly increased the H_0 of WPI and WPI-Trp (Fig. 5A and B), which indicated that the initial interior hydrophobic groups of the natural protein were exposed to the protein surface after pH-shifting. This is also consistent with the increased λ_{max} of WPI and WPI-Trp treated with pH-shifting in the fluorescence spectra. An extremely alkaline pH environment has been shown to result in strong intramolecular electrostatic repulsions of the protein, leading to protein unfolding and a higher surface hydrophobicity (W. Chen et al., 2019; S. Jiang et al., 2017). Meanwhile, WPI and WPI-Trp samples treated with heating also showed increased surface hydrophobicity (Fig. 5A and B). We attribute the increased surface hydrophobicity to the heat treatments changing the spatial structure of the proteins and causing the proteins to unfold and expose hydrophobic groups on the protein surface. This increased surface hydrophobicity

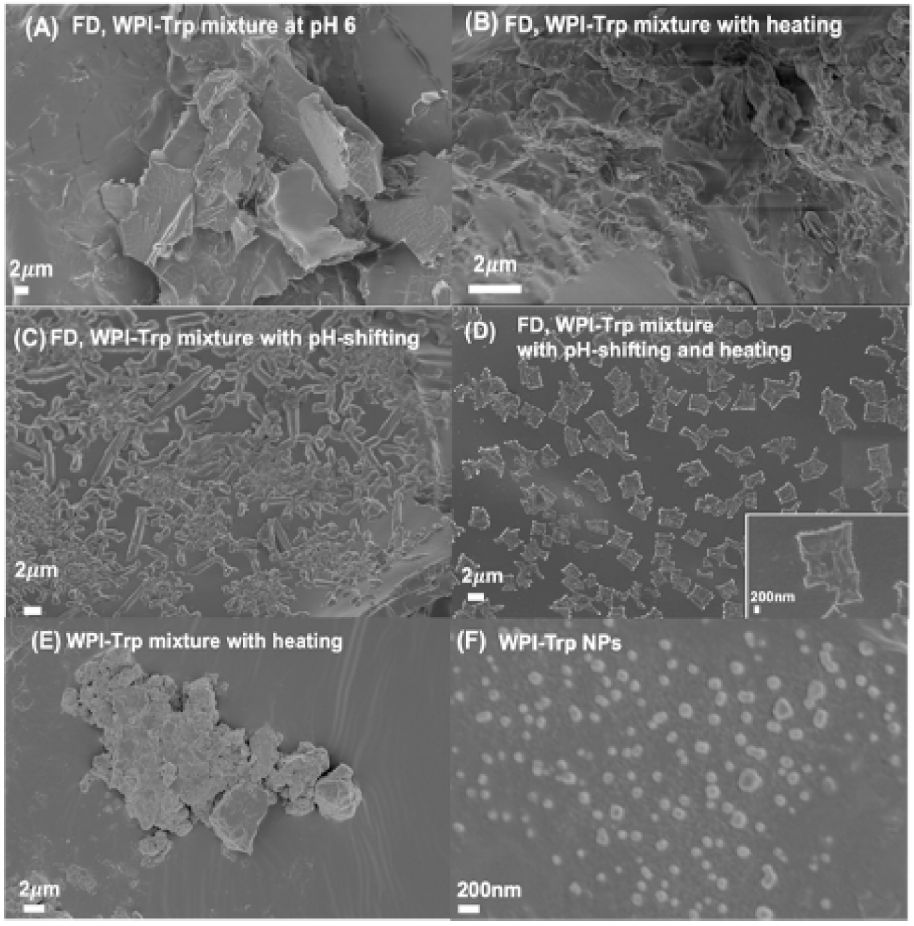

Fig. 4. SEM image of WPI-Trp mixture under different treatments before and after freeze-drying. (A) Freeze-dried WPI-Trp samples at pH 6, (B) Freeze-dried WPI-Trp samples after heat treatment (70 °C, 20 min) at pH 6, (C) Freeze-dried WPI-Trp samples after pH-shifting from 11 to 6, (D) Freeze-dried WPI-Trp samples obtained by pH-shifting from 11 to 6 followed by heat treatment (70 °C, 20 min), (E) WPI-Trp samples after heat treatment (70 °C, 20 min) at pH 6 before freeze-drying, and (F) WPI-Trp NPs before freeze-drying: pH-shifting (from 11 to 6) followed by heat treatment (70 °C, 20 min).

enhances the non-covalent interactions between the WPI-Trp complexes (Y. Wang et al. (2020), Yang, et al., 2020).

The surface hydrophobicity of nanoparticles obtained by pH-shifting combined with heating, however, was lower than the H_0 of pH-shifting alone samples. This was because, after pH-shifting, the protein was in an unstable molten globular state with certain hydrophobic groups exposed, showing a preference for hydrophobic interaction. Therefore, after heating, the exposed hydrophobic groups were buried again, reducing surface hydrophobicity (Raikos, 2010; Ryan & Foegeding, 2015). The aggregation induced by heating might be helpful to the complexation of WPI-Trp NPs. Overall, increased H_0 induced by pH-shifting suggested unfolding and exposure of hydrophobic groups on the WPI, which facilitated the hydrophobic interactions between WPI and Trp during the following heating process.

3.4.3. *Free sulfhydryl group content*

It is believed that the oxidation of SH groups and the interchange between sulfhydryl groups (SH) and disulfide (S-S) bonds play an essential role in protein polymerization (Ryan & Foegeding, 2015; Wouters et al., 2022). Protein species in WPI, β-LG, α-La, and BSA contain 2, 4, and 17 intramolecular S-S bonds, respectively. β-LG and BSA each contain one free thiol (−SH) group (Monahan et al., 1995). Further, SH groups can accept radicals and be oxidized, causing them to be converted to S-S bonds (Y. Wang et al., 2013). After heat treatment on WPI-Trp samples, protein denaturation occurred, and free sulfhydryl groups were exposed, contributing to an increased SH group content (Fig. 5C) (Ji et al., 2022; S. Jiang et al., 2017). More specifically, when β-LG is heated, it separates into monomers, which denature at high temperatures to expose a reactive sulfhydryl group, causing an increased SH group content (Shimada & Cheftel, 1989). Meanwhile, the increase was insignificant ($p > 0.05$) because the oxidation of SH, or interchange SH/S-S reactions, was limited by Trp's antioxidant properties. By contrast, the total SH group content of WPI with heating was significantly lower than natural WPI ($p < 0.05$) (Fig. 5D), which we attribute to the interchange between the oxidation of the −SH or the S-S bond formation induced by heating (Shimada & Cheftel, 1989). Oxidation of SH or conversion of SH into S-S bonding facilitated the polymerization of WPI, as has already been shown in other studies (Gao et al., 2019; S. Jiang et al., 2018; J.-M. Wang et al., 2012).

The −SH group content of WPI significantly increased after pH-shifting ($p < 0.05$) (Fig. 5D), which was related to the unfolding of the protein, suggesting that sulfhydryl groups that were originally buried in the protein were exposed or that disulfide bonds were broken in proteins (Z. Jiang et al., 2022; Y. Wang et al. (2020), Yang, et al., 2020). While −SH content of WPI-Trp with pH-shifting showed no significant difference compared with the untreated WPI-Trp mixture ($p > 0.05$) (Fig. 5C), and this was also related to the reduced oxidation of SH groups in the presence of Trp. WPI-Trp NPs obtained by pH-shifting combined with heating showed the highest SH group content, probably because pH-shifting and heating synergistically enhanced the exposure of the SH group while suppressing the interchange between −SH groups and S-S bond formation due to the presence of Trp. The SH group content of WPI NPs obtained by pH-shifting combined with heating was slightly lower than pH-shifting WPI alone, which was also

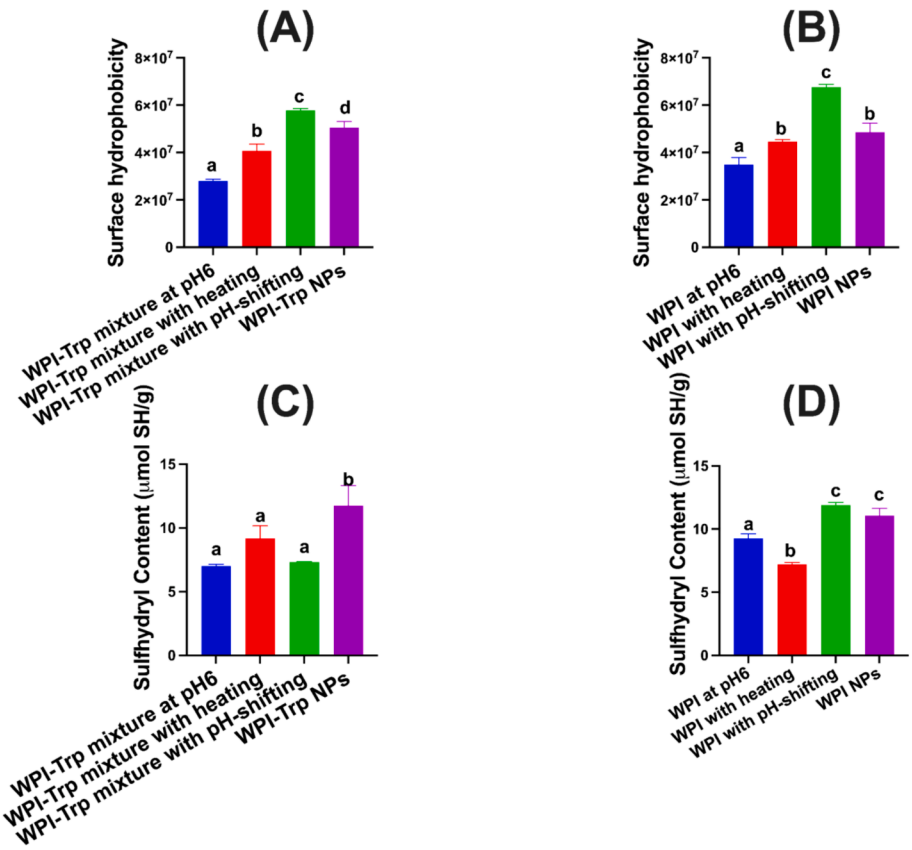

Fig. 5. Surface hydrophobicity (H_0) of WPI-Trp and WPI with different treatments (A) WPI-Trp, and (B) WPI; Free sulfhydryl group content of WPI-Trp and WPI (C) WPI-Trp, and (D) WPI. Different letters indicate a significant difference ($p < 0.05$).

attributed to the oxidation of reactive SH groups or the conversion of SH groups into S-S bonds due to heating. The conversion of SH groups to S-S bonds also contributed to the aggregation of WPI-NPs, as observed in Fig. S1(B). Overall, due to the presence of Trp, oxidation of SH groups to form S-S bonds might be limited during the WPI-Trp NPs formation.

3.4.4. Circular dichroism (CD)

CD spectroscopy was used to identify the secondary structure of WPI and WPI-Trp and analyze the effect of pH-shifting and heating on the secondary structure (Fig. S2 and Table. S1). The untreated WPI exhibited a positive peak at 196 nm for the β-sheet structures and a negative peak at 208 nm for the α-helix structures (Gołębiowski et al., 2020; Y. Wang et al. (2020), Yang, et al., 2020). For WPI and WPI-Trp, both pH-shifting treatment alone and heat treatment alone caused a blue-shift of a minimum of ellipticity (Fig. S2) and thus a decrease of α-helix content (Table. S1), indicating that the WPI protein was unfolded and short peptides were released (C. Zhang et al., 2021). This is consistent with a greater surface hydrophobicity of WPI-Trp and WPI treated by pH-shifting alone or heating alone because small hydrophobic patches were exposed after pH-shifting or heating treatment. The loss of α-helix structure indicated that both heating and pH-shifting caused the protein to reach a molten-globule state with higher flexibility (Z. Jiang et al., 2022; Nicolai et al. 2011a). Specifically, for WPI, both pH-shifting alone and heating alone resulted in a significant decrease in α-helix content ($p < 0.05$) and a significant increase in β-sheet and β-turn ($p < 0.05$). Conversely, WPI-Trp showed neglectable changes in the content of α-helix, β-sheet, and β-turn ($p > 0.05$). This difference was due to the interaction between WPI and Trp, which promoted a more stable secondary structure. The pH-shifting combined with heating treatment further decreased the content of *α*-helix and caused a significant increase in random coil for both WPI-Trp NPs and WPI NPs ($p < 0.05$), suggesting the conversion of α-helix into random coil. This conversion demonstrated a more disordered structure of the modified whey protein with higher flexibility. Previous studies confirm that protein structures are less ordered with increasing content of random coil (W. Chen et al., 2019; H. Jiang et al., 2022; Zhong et al., 2022). In conclusion, both heating and pH-shifting contributed to the disorder of WPI, which the molten-globule state of denatured protein can explain, and the presence of Trp helped stabilize the secondary structure of the protein.

3.4.5. FTIR

FTIR measurement was conducted to analyze the interactions between Trp and WPI, as illustrated in Fig.S3. The amide I band that appeared at 1600–1700 cm^{-1} represented C=O stretching vibrations of the peptide bond. The amide II band was closely related to C–N stretching vibrations and bending vibration of N–H at 1500 cm^{-1}–1600 cm^{-1} (Dai et al., 2017; Zhong et al., 2022). Typical amide I and amide II absorption bands of WPI are located at 1629 cm^{-1}, and 1521 cm^{-1}, respectively. Compared to WPI, the WPI-Trp nanoparticles bands shifted to lower wavenumbers: 1624 cm^{-1} for amide I and 1517 cm^{-1} for amide II. The alteration of amides I and II suggested that hydrophobic interactions between WPI and Trp might occur (Dai et al., 2017). The band in the 3200–3500 cm^{-1} region was associated with the –OH stretching vibrations in protein and indicated hydrogen bonding (Hu et al., 2019; Wei et al., 2021; Zhong et al., 2022). The spectrum of WPI-Trp NPs had a band at 3265 cm^{-1}. Although no significant shifting was observed compared with the WPI, the wider and sharper band between 3200–3500 cm^{-1} of WPI-Trp NPs suggested the formation of hydrogen bonding (Xiao et al., 2015). For Trp, the sharp band at 3394 cm^{-1}, 3010 cm^{-1}, and 742 cm^{-1} corresponded to the N–H stretching vibrations of the indole ring, aromatic C–H stretching vibrations, and C–H bending vibrations in the aromatic ring, respectively (Ivanova, 2006).

After complexation with WPI, the characteristic bands of Trp at 3394 cm^{-1} and 3010 cm^{-1} disappeared, and the intensity of the band at 742

cm^{-1} decreased, indicating interactions between the indole ring and WPI. These interactions were probably related to the hydrogen bonding and the hydrophobic interaction between the indole ring of Trp and WPI. No new bands were detected in the FTIR spectra of WPI-Trp NPs compared with the WPI, suggesting that the interactions between WPI and Trp were mainly non-covalent bonding.

3.4.6. DPPH and ABTS radical scavenging activity of WPI-Trp NPs

Relative ABTS and DPPH radical scavenging capacities of Trp, WPI, and WPI-Trp were measured to assess the impact of pH-shifting and thermal treatments on antioxidant activity (Fig. 6). DPPH is a stable, oil-soluble free radical that can be used to measure radical scavenging activity (Ji et al., 2022). WPI-Trp after heat treatment demonstrated a lower DPPH radical scavenging capacity and showed the lowest DPPH radical scavenging capacity at 5 mg/mL. After heat treatment, the exposed hydrophobic residues and hydrophobic interaction between WPI-Trp particles resulted in aggregation, resulting in low solubility in the DPPH solution. At 5 mg/mL, due to the low solubility of heated WPI-Trp and WPI samples in the DPPH solution, the DPPH radical scavenging capacity was the lowest. The DPPH radical scavenging capacity was not influenced by the pH-shifting treatment of WPI-Trp significantly ($p > 0.05$), while the DPPH scavenging capacity of WPI alone increased significantly ($p < 0.05$).

For the WPI, after pH-shifting treatment, interior amino acids of WPI were exposed, which enhanced the capacity to scavenge free DPPH radicals. For the WPI-Trp NPs obtained by pH-shifting combined with heating, the DPPH scavenging capacity of WPI-Trp was reduced, although the encapsulation of Trp was greatest under these conditions. This may be because the complexation of Trp with WPI stabilized the Trp and blocked access to the DPPH. The reducing effect of DPPH scavenging capacity has been shown in a previous study where the binding of whey protein concentrate with quercetin reduced the DPPH scavenging capacity because the hydrophobic cavity of whey protein concentrates isolated the quercetin from DPPH (Ji et al., 2022).

ABTS radical is water-soluble and can be scavenged by antioxidants when the absorbance of ABTS is reduced (Meira et al., 2012). Due to the difference in solubility, the relative radical scavenging capacity of ABTS was higher than DPPH, and thus, the ABTS radical scavenging capacity was demonstrated at a low sample concentration (0.05 mg/mL). Free Trp showed strong relative ABTS radical scavenging capacity and was not influenced by treatments (Fig. 6F). The ABTS radical scavenging capacity of pH-shifting combined with heating WPI-Trp NPs was significantly lower ($p < 0.05$), suggesting the most significant content of free Trp was encapsulated. The pH-shifting combined with heating treatment was found to induce the strongest complexation of WPI-Trp nanoparticles. Nevertheless, the encapsulation of Trp caused lower antioxidant capacity because it was incorporated within the protein, and steric hindrance inhibited access to the radicals.

3.5. Molecular docking

To investigate the interaction mechanism between Trp and WPI, we used molecular docking. The simulated nanocomplex of WPI-Trp and the three main protein species of WPI were investigated (α-LA, β-LG, and BSA), specifically the optimal docking for hydrogen bonding and hydrophobic interactions (Fig. 7). The amine group in the Trp can form two hydrogen bonds with Glu-49 and Gln-43 residues in α-LA, while other amino acids (Ile-41, Gln −54, His-32, Val-42, Thr-33, Trp-104, Tyr-103, and Phe-53) constituted a hydrophobic pocket to complex with Trp (Fig. 7A). In the case of β-LG, Trp-19 and Glu-44 constituted two hydrogen bonds with the amine group in the indole ring, and Glu-158 formed another hydrogen bond with the amino group of Trp. Amino acid residues of β-LG contributed to the hydrophobic interaction (Thr-18, Tyr-20, Glu-157, Gln-159, and Leu-156) with Trp. In terms of BSA, two hydrogen bonds were formed between the amino acid residues (Leu-189 and Ser-192), and Arg-458, Ile-455, Leu-454, Ala-193, Arg-435, Tyr-451, and Ser-428 were responsible for the hydrophobic interaction during the binding. In terms of the binding affinity (Table. S2), α-LA was predicted to exhibit the highest binding score (−7.9 kcal/mol), followed by BSA (−6.6 kcal/mol) and β-LG (−5.8 kcal/mol), indicating that the α-LA showed the highest binding performance with the Trp. Thus, our molecular docking results suggest that the formation of the WPI-Trp

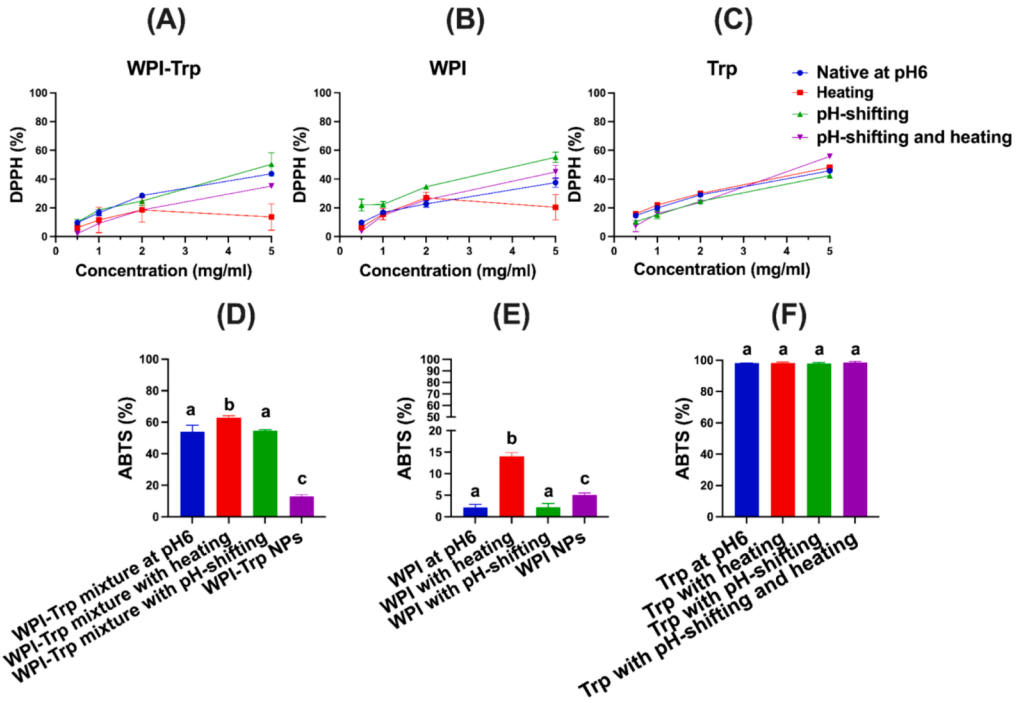

Fig. 6. Antioxidant activity of WPI-Trp, WPI, and Trp with different treatments (A) DPPH radical scavenging capacity of WPI-Trp, (B) DPPH radical scavenging capacity of WPI, (C) DPPH scavenging capacity of Trp, (D) ABTS radical scavenging capacity of WPI-Trp at 0.05 mg/mL, (E) ABTS radical scavenging capacity of WPI at 0.05 mg/mL, and (F) ABTS radical scavenging capacity of Trp at 0.05 mg/mL. Different letters indicate a significant difference ($p < 0.05$).

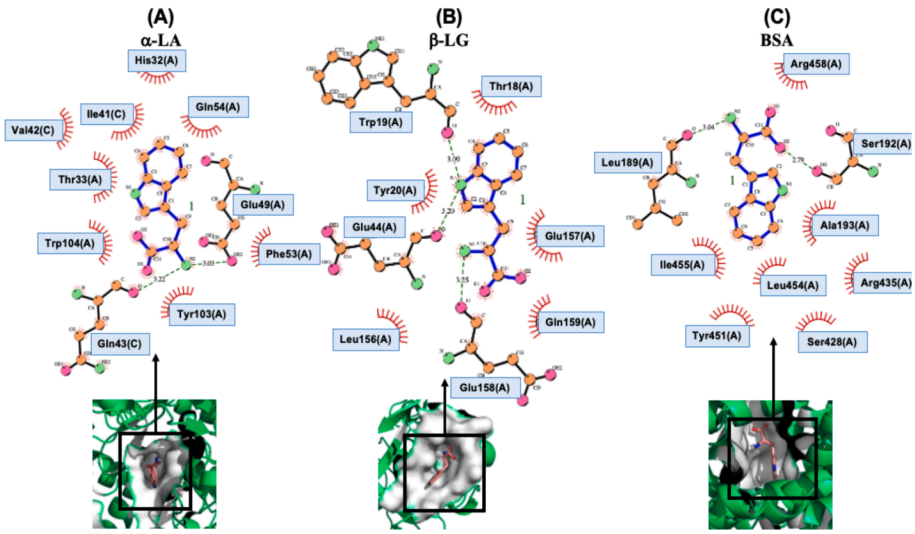

Fig. 7. Molecular docking of complexes (A) α-LA-Trp, (B) β-LG-Trp, and (C) BSA-Trp were shown. Details of binding sites of (A) α-LA-Trp, (B) β-LG-Trp, and (C) BSA-Trp were shown. The green dashed line shows the hydrogen bond. The amino acid residues colored as red indicate hydrophobic interaction with the Trp. (For interpretation of the references to colour in this figure legend, the reader is referred to the web version of this article.)

complex was mainly driven by hydrophobic interactions and hydrogen bonding.

3.6. *Proposed mechanism of the formation of WPI-Trp NPs*

Based on the data we've collected, we propose the following mechanism for the formation of WPI-Trp NPs. The process begins with the unfolding and refolding of whey protein during pH-shifting to place the protein into the molten globule state, where the interior hydrophobic residues are exposed. Among these exposed residues, according to a previous study, Methionine and Proline were prone to bind with Trp (Samanta et al., 2000). Free Trp was then encapsulated into the hydrophobic cavity of the protein. Next, thermal treatment on the WPI-Trp after pH-shifting induced aggregation. During the heating process, whey proteins were denatured, and the interaction between exposed hydrophobic residues, exposure of reactive −SH group, and exchange reactions between −SH and S-S occurred, all of which contributed to the complexation of WPI-Trp NPs (Iametti et al., 1996; Raikos, 2010; Ryan & Foegeding, 2015).

4. Conclusions

The effect on the formation of WPI-Trp nanoparticles of pH-shifting alone, heating alone, and pH-shifting combined with heating was studied. A fluorescence study revealed that pH-shifting and heating under certain conditions produced WPI-Trp nanoparticles. Modifying the WPI structure by thermal and pH-shifting treatment was the main factor for the encapsulation of Trp by WPI. The treatment of pH-shifting encouraged the exposure of hydrophobic residues, including inner fluorophores (Tyrosine, Tryptophan, and Phenylalanine), indicated by the increase of surface hydrophobicity and fluorescence emission maximum. The exposure of hydrophobic residues increased the binding sites for Trp. Heat treatment then encouraged the aggregation of WPI, which was accompanied by increased turbidity and particle size. This process also facilitated the further encapsulation of the added Trp. Based on the aggregation-induced emission, encapsulation of added Trp was confirmed. pH-shifting combined with heat treatment created WPI-Trp nanoparticles that were less thermally sensitive than particles produced through heating alone. Non-covalent interactions, including hydrogen bonding and hydrophobic interaction, were the main driving force for the complexation of WPI-Trp nanoparticles. This study provides a facile, new technique to form WPI-Trp-NPs by pH-shifting followed by heating. The fabrication of these new stable WPI-Trp-NPs extends the application of Trp in dairy products, including whey beverages. For beverage applications, future studies will be focused on scale-up production, assessing sensory characteristics, evaluating storage stability, and investigating thermal stability.

CRediT authorship contribution statement

Lixin Yang: Writing – review & editing, Writing – original draft, Methodology, Investigation, Formal analysis, Data curation, Conceptualization. **Hongmin Dong:** Writing – review & editing, Methodology, Investigation, Conceptualization. **Junyi Wang:** Writing – review & editing, Investigation, Data curation. **Younas Dadmohammadi:** Writing – review & editing, Supervision, Conceptualization. **Yufeng Zhou:** Writing – review & editing, Investigation, Data curation. **Tiantian Lin:** Writing – review & editing, Investigation. **Waritsara Khongkomolsakul:** Writing – review & editing, Investigation. **Gopinathan Meletharayil:** Writing – review & editing, Resources. **Rohit Kapoor:** Writing – review & editing, Resources. **Alireza Abbaspourrad:** Writing – review & editing, Resources, Project administration, Funding acquisition.

Declaration of competing interest

The authors declare that they have no known competing financial interests or personal relationships that could have appeared to influence the work reported in this paper.

Data availability

Data will be made available on request.

Acknowledgments

The authors are grateful for the financial support from Dairy Management, Inc. (Rosemont, IL) The authors would like to thank the assistance and technical support from Dr. Crane and Rebecca Zawistowski in CD spectroscopy. The Cornell Center for Materials Research (CCMR), which is funded by the National Science Foundation (Award Number DMR-1719875), supplied the materials used in this SEM study.

Appendix A. Supplementary data

Supplementary data to this article can be found online at https://doi.org/10.1016/j.foodres.2024.115031.

References

Bhattacharya, M., Jain, N., & Mukhopadhyay, S. (2011). Insights into the Mechanism of Aggregation and Fibril Formation from Bovine Serum Albumin. *The Journal of Physical Chemistry B, 115*(14), 4195–4205. https://doi.org/10.1021/jp111528c

Bromley, E. H. C., Krebs, M. R. H., & Donald, A. M. (2006). Mechanisms of structure formation in particulate gels of β-lactoglobulin formed near the isoelectric point. *The European Physical Journal E, 21*(2), 145–152. https://doi.org/10.1140/epje/i2006-10055-7

Chen, C., Zhong, Q., & Chen, Z. (2022). Improved aqueous solubility, bioaccessibility and cellular uptake of quercetin following pH-driven encapsulation in whey protein isolate. *International Journal of Food Science & Technology, 57*(5), 2747–2755. https://doi.org/10.1111/ijfs.15579

Chen, W., Wang, W., Ma, X., Lv, R., Balaso Watharkar, R., Ding, T., Ye, X., & Liu, D. (2019). Effect of pH-shifting treatment on structural and functional properties of whey protein isolate and its interaction with (−)-epigallocatechin-3-gallate. *Food Chemistry, 274*, 234–241. https://doi.org/10.1016/j.foodchem.2018.08.106

Dai, L., Sun, C., Li, R., Mao, L., Liu, F., & Gao, Y. (2017). Structural characterization, formation mechanism and stability of curcumin in zein-lecithin composite nanoparticles fabricated by antisolvent co-precipitation. *Food Chemistry, 237*, 1163–1171. https://doi.org/10.1016/j.foodchem.2017.05.134

De, S. K., Maity, A., & Chakraborty, A. (2021). Underlying Mechanisms for the Modulation of Self-Assembly and the Intrinsic Fluorescent Properties of Amino Acid-Functionalized Gold Nanoparticles. *Langmuir, 37*(16), 5022–5033. https://doi.org/10.1021/acs.langmuir.1c00431

De Wit, J. N. (2009). Thermal behaviour of bovine β-lactoglobulin at temperatures up to 150°C. a review. *Trends in Food Science & Technology, 20*(1), 27–34. https://doi.org/10.1016/j.tifs.2008.09.012

Delavari, B., Saboury, A. A., Atri, M. S., Ghasemi, A., Bigdeli, B., Khammari, A., Maghami, P., Moosavi-Movahedi, A. A., Haertlé, T., & Goliaei, B. (2015). Alpha-lactalbumin: A new carrier for vitamin D3 food enrichment. *Food Hydrocolloids, 45*, 124–131. https://doi.org/10.1016/j.foodhyd.2014.10.017

Di Pizio, A., & Nicoli, A. (2020). In Silico Molecular Study of Tryptophan Bitterness. *Molecules, 25*(20), 4623. https://doi.org/10.3390/molecules25204623

Ding, S., Ye, X., Qu, L., Mu, J., Huang, L., & Dai, C. (2023). Modification of whey protein isolate by ultrasound-assisted pH shift for complexation with carboxymethylcellulose: Structure and interfacial properties. *International Journal of Biological Macromolecules, 252*, Article 126479. https://doi.org/10.1016/j.ijbiomac.2023.126479

Dong, H., Lin, S., Zhang, Q., Chen, H., Lan, W., Li, H., He, J., & Qin, W. (2016). Effect of extraction methods on the properties and antioxidant activities of Chuanminshen violaceum polysaccharides. *International Journal of Biological Macromolecules, 93*, 179–185. https://doi.org/10.1016/j.ijbiomac.2016.08.074

Dong, H., Yang, L., Dadmohammadi, Y., Li, P., Lin, T., He, Y., Zhou, Y., Li, J., Meletharayil, G., Kapoor, R., & Abbaspourrad, A. (2024). Investigating the synergistic effects of high-pressure homogenization and pH shifting on the formation of tryptophan-rich nanoparticles. *Food Chemistry, 434*, Article 137371. https://doi.org/10.1016/j.foodchem.2023.137371

Friedman, M. (2018). Analysis, Nutrition, and Health Benefits of Tryptophan, 117864691880228 *International Journal of Tryptophan Research, 11*. https://doi.org/10.1177/1178646918802282.

Fuciños, C., Míguez, M., Fuciños, P., Pastrana, L. M., Rúa, M. L., & Vicente, A. A. (2017). Creating functional nanostructures: Encapsulation of caffeine into α-lactalbumin nanotubes. *Innovative Food Science & Emerging Technologies, 40*, 10–17. https://doi.org/10.1016/j.ifset.2016.07.030

Gao, F., Zhang, X., Wang, H., Sun, X., Wang, J., & Wang, C. (2019). Comparison of dry- and wet-heat induced changes in physicochemical properties of whey protein in absence or presence of inulin. *Food Science and Biotechnology, 28*(5), 1367–1374. https://doi.org/10.1007/s10068-019-00577-w

Geddes, C. D. (Ed.). (2016). *Reviews in Fluorescence 2015* (Vol. 8). Springer International Publishing. DOI: 10.1007/978-3-319-24609-3.

Gołębiowski, A., Pomastowski, P., Rodzik, A., Król-Górniak, A., Kowalkowski, T., Górecki, M., & Buszewski, B. (2020). Isolation and Self-Association Studies of Beta-Lactoglobulin. *International Journal of Molecular Sciences, 21*(24), 9711. https://doi.org/10.3390/ijms21249711

Grossmann, L., Beicht, M., Reichert, C., & Weiss, J. (2019). Foaming properties of heat-aggregated microparticles from whey proteins. *Colloids and Surfaces A: Physicochemical and Engineering Aspects, 579*, Article 123572. https://doi.org/10.1016/j.colsurfa.2019.06.037

Hu, Y., Kou, G., Chen, Q., Li, Y., & Zhou, Z. (2019). Protection and delivery of mandarin (Citrus reticulata Blanco) peel extracts by encapsulation of whey protein concentrate nanoparticles. *LWT, 99*, 24–33. https://doi.org/10.1016/j.lwt.2018.09.044

Iametti, S., Gregori, B., Vecchio, G., & Bonomi, F. (1996). Modifications Occur at Different Structural Levels During the Heat Denaturation of beta-Lactoglobulin. *European Journal of Biochemistry, 237*(1), 106–112. https://doi.org/10.1111/j.1432-1033.1996.0106n.x

Igartúa, D. E., Dichano, M. C., Ferrari, S. B., Palazolo, G. G., & Cabezas, D. M. (2024). Combination of pH-shifting, ultrasound, and heat treatments to enhance solubility and emulsifying stability of rice protein isolate. *Food Chemistry, 433*, Article 137319. https://doi.org/10.1016/j.foodchem.2023.137319

Ivanova, B. B. (2006). IR-LD spectroscopic characterization of l-Tryptophan containing dipeptides. *Spectrochimica Acta Part A: Molecular and Biomolecular Spectroscopy, 64*(4), 931–938. https://doi.org/10.1016/j.saa.2005.08.022

Jain, A., Singh, S. K., Arya, S. K., Kundu, S. C., & Kapoor, S. (2018). Protein Nanoparticles: Promising Platforms for Drug Delivery Applications. *ACS Biomaterials Science & Engineering, 4*(12), 3939–3961. https://doi.org/10.1021/acsbiomaterials.8b01098

Ji, W., Yang, F., & Yang, M. (2022). Effect of change in pH, heat and ultrasound pre-treatments on binding interactions between quercetin and whey protein concentrate. *Food Chemistry, 384*, Article 132508. https://doi.org/10.1016/j.foodchem.2022.132508

Jiang, H., Pan, J., Hu, X., Zhu, M., Gong, D., & Zhang, G. (2022). A combination of alkaline pH-shifting/acidic pH and thermal treatments improves the solubility and emulsification properties of wheat glutenin. *Food Chemistry, 393*, Article 133358. https://doi.org/10.1016/j.foodchem.2022.133358

Jiang, J., Wang, Q., & Xiong, Y. L. (2018). A pH shift approach to the improvement of interfacial properties of plant seed proteins. *Current Opinion in Food Science, 19*, 50–56. https://doi.org/10.1016/j.cofs.2018.01.002

Jiang, J., Xiong, Y. L., & Chen, J. (2010). pH Shifting Alters Solubility Characteristics and Thermal Stability of Soy Protein Isolate and Its Globulin Fractions in Different pH, Salt Concentration, and Temperature Conditions. *Journal of Agricultural and Food Chemistry, 58*(13), 8035–8042. https://doi.org/10.1021/jf101045b

Jiang, S., Altaf hussain, M., Cheng, J., Jiang, Z., Geng, H., Sun, Y., Sun, C., & Hou, J. (2018). Effect of heat treatment on physicochemical and emulsifying properties of polymerized whey protein concentrate and polymerized whey protein isolate. *LWT, 98*, 134–140. DOI: 10.1016/j.lwt.2018.08.028.

Jiang, S., Ding, J., Andrade, J., Rababah, T. M., Almajwal, A., Abulmeaty, M. M., & Feng, H. (2017). Modifying the physicochemical properties of pea protein by pH-shifting and ultrasound combined treatments. *Ultrasonics Sonochemistry, 38*, 835–842. https://doi.org/10.1016/j.ultsonch.2017.03.046

Jiang, Z., Gao, Y., Li, J., Wang, K., Ma, C., Sun, D., Hussain, M. A., Qayum, A., & Hou, J. (2022). Consecutive pH-shift and ultrasound treatment modify the physicochemical properties of whey protein isolate. *International Dairy Journal, 127*, Article 105211. https://doi.org/10.1016/j.idairyj.2021.105211

Julieta, F. R. M., Macarena, S., Daniela, I., Jimena, P. M., Valle, A. S. D., & Silvia, C. N. (2013). Lipid-Polymer Membranes as Carriers for L-Tryptophan: Molecular and Metabolic Properties. *Open Journal of Medicinal Chemistry, 03*(01), 31–39. https://doi.org/10.4236/ojmc.2013.31005

Li, X., Wang, G., Chen, D., & Lu, Y. (2015). β-Carotene and astaxanthin with human and bovine serum albumins. *Food Chemistry, 179*, 213–221. https://doi.org/10.1016/j.foodchem.2015.01.133

Lin, T., Dadmohammadi, Y., Davachi, S. M., Torabi, H., Li, P., Pomon, B., Meletharayil, G., Kapoor, R., & Abbaspourrad, A. (2022). Improvement of lactoferrin thermal stability by complex coacervation using soy soluble polysaccharides. *Food Hydrocolloids, 131*, Article 107736. https://doi.org/10.1016/j.foodhyd.2022.107736

Liu, Q., Sun, Y., Cheng, J., & Guo, M. (2022). Development of whey protein nanoparticles as carriers to deliver soy isoflavones. *LWT, 155*, Article 112953. https://doi.org/10.1016/j.lwt.2021.112953

Liu, Y., Wolstenholme, C. H., Carter, G. C., Liu, H., Hu, H., Grainger, L. S., Miao, K., Fares, M., Hoelzel, C. A., Yennawar, H. P., Ning, G., Du, M., Bai, L., Li, X., & Zhang, X. (2018). Modulation of Fluorescent Protein Chromophores To Detect Protein Aggregation with Turn-On Fluorescence. *Journal of the American Chemical Society, 140*(24), 7381–7384. https://doi.org/10.1021/jacs.8b02176

Matsarskaia, O., Bühl, L., Beck, C., Grimaldo, M., Schweins, R., Zhang, F., Seydel, T., Schreiber, F., & Roosen-Runge, F. (2020). Evolution of the structure and dynamics of bovine serum albumin induced by thermal denaturation. *Physical Chemistry Chemical Physics, 22*(33), 18507–18517. https://doi.org/10.1039/D0CP01857K

McGuffey, M. K., Epting, K. L., Kelly, R. M., & Foegeding, E. A. (2005). Denaturation and Aggregation of Three α-Lactalbumin Preparations at Neutral pH. *Journal of Agricultural and Food Chemistry, 53*(8), 3182–3190. https://doi.org/10.1021/jf048863p

Meira, S. M. M., Daroit, D. J., Helfer, V. E., Corrêa, A. P. F., Segalin, J., Carro, S., & Brandelli, A. (2012). Bioactive peptides in water-soluble extracts of ovine cheeses from Southern Brazil and Uruguay. *Food Research International, 48*(1), 322–329. https://doi.org/10.1016/j.foodres.2012.05.009

Mohammadian, M., Moghadam, M., Salami, M., Emam-Djomeh, Z., Alavi, F., Momen, S., & Moosavi-Movahedi, A. A. (2020). Whey protein aggregates formed by non-toxic chemical cross-linking as novel carriers for curcumin delivery: Fabrication and characterization. *Journal of Drug Delivery Science and Technology, 56*, Article 101531. https://doi.org/10.1016/j.jddst.2020.101531

Monahan, F. J., German, J. B., & Kinsella, J. E. (1995). Effect of pH and temperature on protein unfolding and thiol/disulfide interchange reactions during heat-induced gelation of whey proteins. *Journal of Agricultural and Food Chemistry, 43*(1), 46–52. https://doi.org/10.1021/jf00049a010

Nayak, B. N., & Buttar, H. S. (2016). Evaluation of the antioxidant properties of tryptophan and its metabolites in *in vitro* assay. *Journal of Complementary and Integrative Medicine, 13*(2), 129–136. https://doi.org/10.1515/jcim-2015-0051

Nicolai, T., Britten, M., & Schmitt, C. (2011). β-Lactoglobulin and WPI aggregates: Formation, structure and applications. *Food Hydrocolloids, 25*(8), 1945–1962. https://doi.org/10.1016/j.foodhyd.2011.02.006

Nongonierma, A. B., & FitzGerald, R. J. (2015). Milk proteins as a source of tryptophan-containing bioactive peptides. *Food & Function, 6*(7), 2115–2127. https://doi.org/10.1039/C5FO00407A

Raikos, V. (2010). Effect of heat treatment on milk protein functionality at emulsion interfaces. *A review. Food Hydrocolloids, 24*(4), 259–265. https://doi.org/10.1016/j.foodhyd.2009.10.014

Roy, I., & Gupta, M. N. (2004). Freeze-drying of proteins: Some emerging concerns. *Biotechnology and Applied Biochemistry, 39*(2), 165. https://doi.org/10.1042/BA20030133

Royer, C. A. (2006). Probing Protein Folding and Conformational Transitions with Fluorescence. *Chemical Reviews, 106*(5), 1769–1784. https://doi.org/10.1021/cr0404390

Rudolph, S., Riedel, E., & Henle, T. (2018). Studies on the interaction of the aromatic amino acids tryptophan, tyrosine and phenylalanine as well as tryptophan-containing dipeptides with cyclodextrins. *European Food Research and Technology, 244*(9), 1511–1519. https://doi.org/10.1007/s00217-018-3065-9

Ryan, K. N., & Foegeding, E. A. (2015). Formation of soluble whey protein aggregates and their stability in beverages. *Food Hydrocolloids, 43*, 265–274. https://doi.org/10.1016/j.foodhyd.2014.05.025

Saberi Riseh, R., Gholizadeh Vazvani, M., Hassanisaadi, M., Thakur, V. K., & Kennedy, J. F. (2023). Use of whey protein as a natural polymer for the encapsulation of plant biocontrol bacteria: A review. *International Journal of Biological Macromolecules, 234*, Article 123708. https://doi.org/10.1016/j.ijbiomac.2023.123708

Salleh, N., Goh, K. K. T., Waterland, M. R., Huffman, L. M., Weeks, M., & Matia-Merino, L. (2022). Complexation of Anthocyanin-Bound Blackcurrant Pectin and Whey Protein: Effect of pH and Heat Treatment. *Molecules, 27*(13), 4202. https://doi.org/10.3390/molecules27134202

Samanta, U., Pal, D., & Chakrabarti, P. (2000). Environment of tryptophan side chains in proteins. *Proteins: Structure, Function, and Genetics, 38*(3), 288–300. https://doi.org/10.1002/(SICI)1097-0134(20000215)38:3<288::AID-PROT5>3.0.CO;2-7

Saokham, P., Muankaew, C., Jansook, P., & Loftsson, T. (2018). Solubility of Cyclodextrins and Drug/Cyclodextrin Complexes. *Molecules, 23*(5), 1161. https://doi.org/10.3390/molecules23051161

Shakoury, N., Aliyari, M. A., Salami, M., Emam-Djomeh, Z., Vardhanabhuti, B., & Moosavi-Movahedi, A. A. (2022). Encapsulation of propolis extract in whey protein nanoparticles. *LWT, 158*, Article 113138. https://doi.org/10.1016/j.lwt.2022.113138

Shimada, K., & Cheftel, J. C. (1989). Sulfhydryl group/disulfide bond interchange reactions during heat-induced gelation of whey protein isolate. *Journal of Agricultural and Food Chemistry, 37*(1), 161–168. https://doi.org/10.1021/jf00085a038

Sun, Y., Chen, H., Chen, W., Zhong, Q., shen, Y., & Zhang, M. (2022). Effect of ultrasound on pH-shift to improve thermal stability of coconut milk by modifying physicochemical properties of coconut milk protein. *LWT*, *167*, 113861. DOI: 10.1016/j.lwt.2022.113861.

Tang, C. (2021). Assembled milk protein nano-architectures as potential nanovehicles for nutraceuticals. *Advances in Colloid and Interface Science, 292*, Article 102432. https://doi.org/10.1016/j.cis.2021.102432

Tang, Z., Ying, R., & Shi, L. (2021). Physicochemical and functional characteristics of proteins treated by a pH-shift process: A review. *International Journal of Food Science & Technology, 56*(2), 515–529. https://doi.org/10.1111/ijfs.14758

Trott, O., & Olson, A. J. (2009). AutoDock Vina: Improving the speed and accuracy of docking with a new scoring function, efficient optimization, and multithreading. *Journal of Computational Chemistry, NA-NA.*. https://doi.org/10.1002/jcc.21334

Wallace, A. C., Laskowski, R. A., & Thornton, J. M. (1995). LIGPLOT: A program to generate schematic diagrams of protein-ligand interactions. *Protein Engineering, Design and Selection, 8*(2), 127–134. https://doi.org/10.1093/protein/8.2.127

Wang, C., Cui, B., Sun, Y., Wang, C., & Guo, M. (2022). Preparation, stability, antioxidative property and in vitro release of cannabidiol (CBD) in zein-whey protein composite nanoparticles. *LWT, 162*, Article 113466. https://doi.org/10.1016/j.lwt.2022.113466

Wang, J.-M., Xia, N., Yang, X.-Q., Yin, S.-W., Qi, J.-R., He, X.-T., Yuan, D.-B., & Wang, L.-J. (2012). Adsorption and Dilatational Rheology of Heat-Treated Soy Protein at the Oil-Water Interface: Relationship to Structural Properties. *Journal of Agricultural and Food Chemistry, 60*(12), 3302–3310. https://doi.org/10.1021/jf205128v

Wang, R., Zeng, M.-Q., Wu, Y.-W., Teng, Y.-X., Wang, L.-H., Li, J., Xu, F.-Y., Chen, B.-R., Han, Z., & Zeng, X.-A. (2023). Enhanced encapsulation of lutein using soy protein isolate nanoparticles prepared by pulsed electric field and pH shifting treatment. *Food Chemistry, 424*, Article 136386. https://doi.org/10.1016/j.foodchem.2023.136386

Wang, Y., Xiong, Y. L., Rentfrow, G. K., & Newman, M. C. (2013). Oxidation promotes cross-linking but impairs film-forming properties of whey proteins. *Journal of Food Engineering, 115*(1), 11–19. https://doi.org/10.1016/j.jfoodeng.2012.09.013

Wang, Y., Yang, F., Wu, M., Li, J., Bai, Y., Xu, W., & Qiu, S. (2020). Synergistic effect of pH shifting and mild heating in improving heat induced gel properties of peanut protein isolate. *LWT, 131*, Article 109812. https://doi.org/10.1016/j.lwt.2020.109812

Wang, Y., Zhang, L., Wang, P., Xu, X., & Zhou, G. (2020). pH-shifting encapsulation of curcumin in egg white protein isolate for improved dispersity, antioxidant capacity and thermal stability. *Food Research International, 137*, Article 109366. https://doi.org/10.1016/j.foodres.2020.109366

Wei, Y., Zhan, X., Dai, L., Zhang, L., Mao, L., Yuan, F., Liu, J., & Gao, Y. (2021). Formation mechanism and environmental stability of whey protein isolate-zein core-shell complex nanoparticles using the pH-shifting method. *LWT, 139*, Article 110605. https://doi.org/10.1016/j.lwt.2020.110605

Wouters, A. G. B., Boeve, J., Dams, H., & Joye, I. J. (2022). Heat treatment as a food-grade strategy to increase the stability of whey protein particles under food system relevant conditions. *Food Hydrocolloids, 124*, Article 107254. https://doi.org/10.1016/j.foodhyd.2021.107254

Xiao, J., Nian, S., & Huang, Q. (2015). Assembly of kafirin/carboxymethyl chitosan nanoparticles to enhance the cellular uptake of curcumin. *Food Hydrocolloids, 51*, 166–175. https://doi.org/10.1016/j.foodhyd.2015.05.012

Xue, C., Li, G., Zheng, Q., Gu, X., Shi, Q., Su, Y., Chu, Q., Yuan, X., Bao, Z., Lu, J., & Li, L. (2023). Tryptophan metabolism in health and disease. *Cell Metabolism, 35*(8), 1304–1326. https://doi.org/10.1016/j.cmet.2023.06.004

Yi, J., Fan, Y., Yokoyama, W., Zhang, Y., & Zhao, L. (2016). Characterization of milk proteins–lutein complexes and the impact on lutein chemical stability. *Food Chemistry, 200*, 91–97. https://doi.org/10.1016/j.foodchem.2016.01.035

Yu, Y., Gong, Q.-T., Lu, W.-F., Liu, Y.-H., Yang, Z.-J., Wang, N., & Yu, X.-Q. (2020). Aggregation-Induced Emission Probes for Specific Turn-On Quantification of Bovine Serum Albumin. *ACS Applied Bio Materials, 3*(8), 5193–5201. https://doi.org/10.1021/acsabm.0c00589

Zhan, F., Ding, S., Xie, W., Zhu, X., Hu, J., Gao, J., Li, B., & Chen, Y. (2020). Towards understanding the interaction of β-lactoglobulin with capsaicin: Multi-spectroscopic, thermodynamic, molecular docking and molecular dynamics simulation approaches. *Food Hydrocolloids, 105*, Article 105767. https://doi.org/10.1016/j.foodhyd.2020.105767

Zhang, C., Fu, Y., Li, Z., Li, T., Shi, Y., Xie, H., Li, Y., Su, H., & Li, Z. (2021). Application of whey protein isolate fibrils in encapsulation and protection of β-carotene. *Food Chemistry, 346*, Article 128963. https://doi.org/10.1016/j.foodchem.2020.128963

Zhang, L., Zhou, R., Zhang, J., & Zhou, P. (2021). Heat-induced denaturation and bioactivity changes of whey proteins. *International Dairy Journal, 123*, Article 105175. https://doi.org/10.1016/j.idairyj.2021.105175

Zhang, Z., Li, Y., Lee, M. C., Ravanfar, R., Padilla-Zakour, O. I., & Abbaspourrad, A. (2020). The Impact of High-Pressure Processing on the Structure and Sensory Properties of Egg White-Whey Protein Mixture at Acidic Conditions. *Food and Bioprocess Technology, 13*(2), 379–389. https://doi.org/10.1007/s11947-019-02397-6

Zhao, C., Chen, N., & Ashaolu, T. J. (2022). Whey proteins and peptides in health-promoting functions – A review. *International Dairy Journal, 126*, Article 105269. https://doi.org/10.1016/j.idairyj.2021.105269

Zhong, M., Sun, Y., Sun, Y., Fang, L., Wang, Q., Qi, B., & Li, Y. (2022). Soy lipophilic protein self-assembled by pH-shift combined with heat treatment: Structure, hydrophobic resveratrol encapsulation, emulsification, and digestion. *Food Chemistry, 394*, Article 133514. https://doi.org/10.1016/j.foodchem.2022.133514

Zhu, J., Sun, X., Wang, S., Xu, Y., & Wang, D. (2017). Formation of nanocomplexes comprising whey proteins and fucoxanthin: Characterization, spectroscopic analysis, and molecular docking. *Food Hydrocolloids, 63*, 391–403. https://doi.org/10.1016/j.foodhyd.2016.09.027